PRODUCTION AND CHARACTERIZATION OF ACTIVATED CARBON DERIVED FROM ORANGE PEEL FOR THE ADSORPTION OF METHYLENE BLUE DYE

[1]Esther Baba, [2]Gideon Wyasu, [1]Ayoola Joseph Adefila, Nathan A. Dikko[2]* and Jamila B. Yakasai[3]

[1]Department of Chemistry, Ahmadu Bello University, Zaria, Kaduna State, Nigeria
[2]Department of Pure and Applied Chemistry, Faculty of Physical Sciences, Kaduna State University, Kaduna State, Nigeria
[3]National Water Resources Institute, Mando – Kaduna.

*Corresponding Author Email Address: nathandikko2.@gmail.com

ABSTRACT
Activated carbon was produced from orange peel using H_2SO_4 and $ZnCl_2$ as activating agents at a temperature of 400 °C. The impregnation was done in 1:1 (wt/v). FTIR analysis of the precursor and activated carbon shows different functional groups present in the precursor and activated carbon. The FTIR spectral also shows shifts in bands and changes in wave number between the precursor and activated carbon indicating chemical transformation during activation and carbonization. SEM analysis was used to study the internal structure and pores development of the activated carbon. The methylene blue adsorption capacity of the activated carbon was determined using standard methods. Langmuir and Freundlich adsorption isotherms were employed in determining the adsorption process and Pseudo first-order and Pseudo second-order kinetics were employed in determining the rate of adsorption by the adsorbents.

Keywords: Activated carbon, orange peel, adsorption isotherms, Langmuir, Freundlich, adsorption kinetics.

1. INTRODUCTION
Activated carbons (AC) are porous and adsorbent materials, the significance and relevance of activated carbon to a rapidly developing society cannot be overstated with its' numerous applications ranging from liquid phase to gaseous phase (Yusufu *et al.,* 2012). AC derived from agricultural by-products has the edge of being a cost-effective replacement for non-renewable coal-based granular activated carbons (GACs), as long as they have comparable or greater adsorption efficiency. Agricultural byproducts are a good source of raw materials for the manufacturing of activated carbon due to their abundance and availability (Sugumaran *et al.,* 2012). The capacity and selectivity of activated carbon as an adsorbent are determined by the degree of disorganization of the microcrystalline structure, which is influenced by both the nature of the precursor material and the process through which it was transformed into activated carbon (Pallarés *et al.,* 2018). Chemical and physical activation processes can be used to produce AC. In many instances, chemical activation provides several benefits, such as lowering activation temperature and providing well-developed porosity through the use of diverse activating chemicals (Özsin *et al.,* 2019). H_2SO_4 and $ZnCl_2$ have been increasingly utilized as activation reagents, resulting in high specific surface area of the produced ACs (Evwierhoma *et al.,* 2018)

Managing the contamination of wastewater by dye molecules has gained significance in order to minimize the environmental consequences. Methylene blue (MB) is a widely utilized thiazine dye in various industries, owing to its chemical stability and water solubility, which are attributed to its molecular structure. It is characterized by the chemical formula $C_{16}H_{18}N_3ClS$ (Xue *et al.* 2022). Earlier research has indicated that contact with methylene blue (MB) can lead to eye injuries and skin damage. Furthermore, direct ingestion of MB has been associated with symptoms such as elevated heart rate, digestive disorders, nausea, vomiting, and tissue necrosis (Egbosiuba *et al.,* 2020). Public health and environmental authorities express concern over the aesthetic colouration caused by the presence of dyes and pigments in wastewater, even when released in small quantities into the environment (Jawad *et al.,* 2016). Activated carbon is widely recognized as a common and effective adsorbent employed for the removal of dyes from waste water due to its extensive surface area, high adsorption capacity and diversity of functional groups (Islam *et al.,* 2017). Hence, it is important to develop a highly effective and advance treatment approach for the removal of MB. This is crucial in ensuring the preservation of a safe and healthy environment.

Orange is a citrus plant of the Rutaceae family that is widely cultivated and processed around the world for the manufacturing of a variety of products, including orange juice, which is related with the production of a relatively high volume of orange peel. This byproduct is occasionally dumped as waste in the environment (Gavahian *et al.,* 2019). According to Martín *et al.* (2010), global orange production was projected to be 63,906,094 tons in 2007. A large portion of this production (70%) is used to make products like juice or marmalade. Furthermore, 50-60% of the processed fruit is converted into citrus peel waste. The tons of Orange peels are discarded and send garbage as useless material and it is very essential to find applications and uses for these peels as a management of waste now days is becoming a very serious environment issue. The orange peel waste peels are low cost, non-hazardous and environmental friendly biomaterials which can be used as adsorbent in various applications (Santos *et al.,* 2015). In the present study, we report the production of AC from orange peel waste using H_2SO_4 and $ZnCl_2$ and its characterization and adsorption capacity.

2.0 MATERIALS AND METHODS
2.1 Source/sample Preparation
Orange peels were obtained from Sabo market Chikun Local Government and Monday Market at Kakuri, Kaduna South Local

Government. The orange peels were cut into smaller sizes and washed with de-ionized water. The washed orange peels were sun dried for 7days; the pieces were then dried in an oven at 110 °C. The dried orange peels were pulverized using a clean pestle and mortar to reduce it to different particle sizes. The crushed orange peels were sieved to the require particle size of 400 μm and 850 μm using a vibrator with sieve tray of different mesh size.

2.2 Preparation of Activated Carbon
Chemical activation and carbonization with $ZnCl_2$ and H_2SO_4 was carried out as described by Wyasu (2020). 30 g of the precursor (400 μm) and 50 g of the precursor (850 μm) was weighed inside the crucible, and the precursor was impregnated with 1 M of sulphuric acid (H_2SO_4) and 1 M $ZnCl_2$. The impregnation was carried out by soaking the precursor with 30 cm^3 and 50 cm^3 of the activating agent (H_2SO_4 and $ZnCl_2$) respectively, at ratio 1:1 (w/v). The mixture was then dried in an oven for 3 h at 110 °C. The carbonization process was carried out in the furnace at 400 °C for 2 h. The activated carbon produced was cooled and washed several times with de-ionized water until it is neutral (colourless) to litmus paper. The final activated carbon was then dried in an oven for 1 h at 110 °C, cooled in a desiccator and stored in air tight bottles.
The activated carbon yield was calculated using the formula;

$$X\ (\%) = \frac{m}{m_o} \times 100 \qquad (1)$$

Where X (%) is the activated carbon yield, m is the mass of activated carbon and m_o is the raw mass of the precursor.

2.3 Surface Characterization of Adsorbent

2.3.1 Fourier Transformed Infrared Spectroscopy (FTIR)
The surface functional groups of the precursor and activated carbon were characterized using a Perkin Elmer, USA FT-IR spectrophotometer. To determine the FTIR spectra the method by Wibawa *et al.* (2020) was used. The samples were mixed with KBr pellets for FTIR analysis. The infrared spectra were recorded in the range of 4000-750 cm^{-1}. To identify the functional groups and covalent bonds vibration type present in the sample, the spectral data were compared to a reference.

2.3.2 Scanning Electron Microscope Analysis (SEM)
The surface morphology of the precursor and activated carbon were investigated using a scanning electron microscope (Hitachi, Japan) based on methods described by Wibawa *et al.* (2020).

2.4 Adsorption Studies
Adsorption equilibrium and kinetics were determined by the batch method according to Ünal *et al.* (2013). The stock solution (1000 mgL^{-1}) was prepared by dissolving the 1000 mg of MB in 1.0 L of distilled water. Adsorption isotherms were performed in a series of 50 mL conical flasks where dye solutions (10 mL) with different initial concentrations (2–10 ppm) at pH 6.5. 0.1 g of activated carbon was added to the solution and then stirred at 150 rpm for 2 h at room temperature. It was then filtered and the absorbance of the filtrate was taken using an Agilent 2344 spectrophotometer at wavelength (λ) 670 nm.
Kinetic experiments followed essentially the same procedures as equilibrium tests. The aqueous samples were collected at specific time intervals ranging from 30 – 75 minutes. Every kinetic experiment was conducted with 10 ppm of dye concentration at room temperature and the dye concentrations after adsorption were measured in a similar manner.
The adsorption capacity at equilibrium (q_e) and adsorption capacity at any time (q_t), were determined by equations (2) and (3) respectively;

$$q_e(mgg^{-1}) = \frac{(Co-Ce)V}{m} \qquad (2)$$

$$q_t(mgg^{-1}) = \frac{(Co-Ct)V}{m} \qquad (3)$$

where, C_e is equilibrium concentration of methylene blue, C_t is the concentration of methylene blue at any time, C_o is the initial concentration of methylene blue, V is the volume of methylene blue used (L), and m is the mass of activated carbon used (g).

3.0 RESULTS AND DISCUSSION

3.1 Percentage Yield of Activated carbon
The percentage yield of activated carbon is presented in Table 1. The result shows that particle size affects the yield, the bigger the particle size, the higher the yield. Activated carbon produced from orange peel using $ZnCl_2$ as activating agent gives better yield (58.50 % for 850 μm and 48.50 % for 400 μm) than H_2SO_4 (49.16 % for 850 μm and 45.72 % for 400 μm).

Table 1: Percentage yield of activated carbon produced from orange peel

Activating agents	Particle size of precursor (μm)	Weight of precursor (g)	Weight of activated carbon (g)	Percentage yield of activated carbon (%)
H_2SO_4	850	50	24.580	49.16
H_2SO_4	400	30	13.715	45.72
$ZnCl_2$	850	50	29.250	58.50
$ZnCl_2$	400	30	14.550	48.50

3.2 FTIR Spectral of Raw Orange Peel (precursor) and Activated Carbons
The functional groups of the raw orange peel and activated carbon produced from the FTIR spectra of the orange peel activated carbons (OP-AC) are presented in Figures 1, 2 and 3
The surface functional groups present in the precursor were the band corresponding to O-H group in alcohol at 3650 cm^{-1}; a band at 2950-2800 cm^{-1} corresponded to C-C stretch in alkanes; the band at 1525 cm^{-1} was caused due to the presence of aromatic nitro compounds; C-H bend was observed at 1450-1470 cm^{-1} due to the presence of C-H bend in alkanes and alkyls; the band at 1050-1150 cm^{-1} corresponded to C-O group in alkoxyl; the band at 2260-2210 cm^{-1} was ascribed to C≡N in Nitriles; and the band at 1740-1755 cm^{-1} corresponded to C=O stretch in carbonyls.
The spectra at Figure 2 and 3 showed that some peaks were shifted or disappeared while some new peaks were also detected which may be attributed to the activation process. The surface functional groups present in the H_2SO_4 activated carbon were the band corresponding to O-H group in alcohol at 3300-3400 cm^{-1}; the peak at 2260-2210 cm^{-1} was ascribed to C≡N in nitriles. The peak at 1640-1690 cm^{-1} corresponded to C=O stretch in amide; the band at 1450-1470 cm^{-1} was ascribed to C-H bend in alkanes and alkyls; C-H bend in aromatic compounds were observed at 810-840 cm^{-1}. The surface functional groups present in the $ZnCl_2$ activated carbon were the peak corresponding to O-H groups in alcohol at 3300-3400 cm^{-1}; the band at 1640-1690 cm^{-1} corresponded to C=O

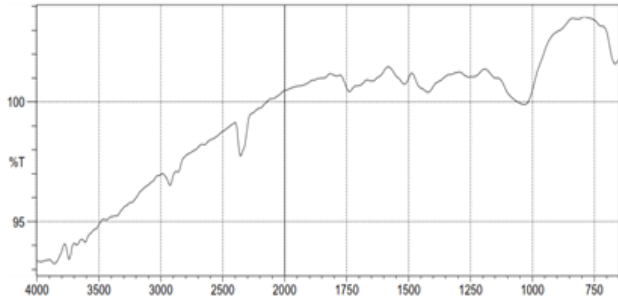stretch in amide; the band at 1035-1050 cm^{-1} were ascribed to C-O stretch in alcohol.
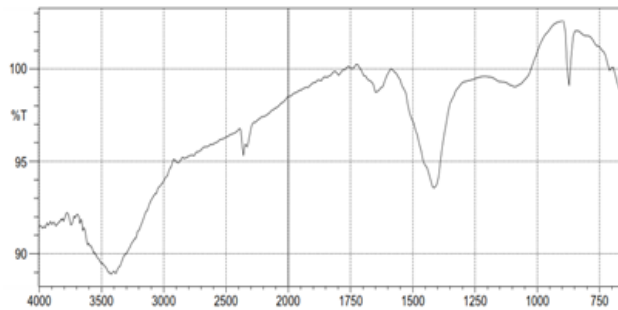

Figure 1: FTIR Spectral of orange peel (precursor)

Figure 2: FTIR Spectral of H_2SO_4 activated carbon

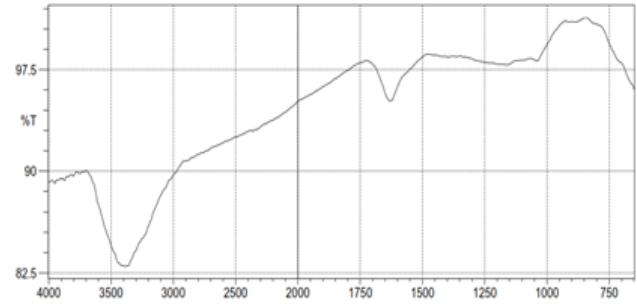**Figure 3:** FTIR Spectral of $ZnCl_2$ activated carbon

3.3 SEM Micrograph of Precursor and Activated Carbon

The surface morphology of the raw orange peel (precursor) and activated carbons from the orange peel are presented in plate 1. Plate 1 shows the SEM result for the precursor (A), H_2SO_4 activated carbon (B) and $ZnCl_2$ activated carbon (C). The SEM micrograph in plate 1 shows that the surface morphology of the precursor has poorly developed pores. However, it was observed in plate B and C that activation and carbonization processes had a strong influence on the external structure of the precursor after chemical activation and carbonization.
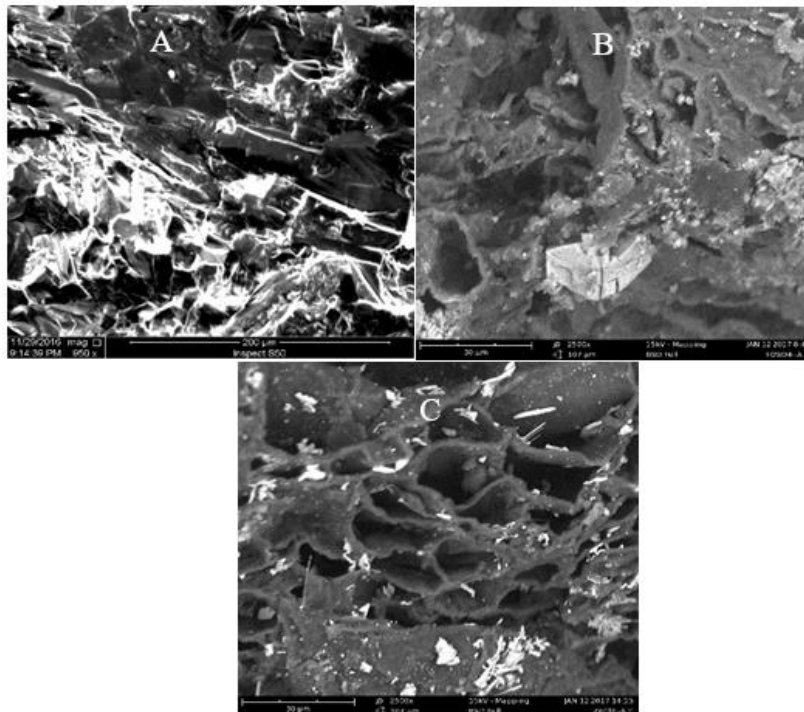

Plate 1: SEM micrograph for precursor (orange peel) (A), H_2SO_4 activated carbon (B), and $ZnCl_2$ activated carbon (C)

The porous activated carbons from the precursor had rough eroded surface, holes and cave like opening. The surface morphology shows that the pores were more pronounced when the precursors were subjected to treatment with activating agent (H_2SO_4 and $ZnCl_2$). The result has shown that the activated carbon produced using $ZnCl_2$ as activating agent has better developed pores.

3.4 Adsorption Studies

3.4.1 Langmuir Adsorption Isotherm

Table 2: Adsorption equilibrium studies for the removal of methylene blue by OP-AC activated with H_2SO_4 and $ZnCl_2$

H_2SO_4			$ZnCl_2$		
C_o	C_e	q_e	C_o	C_e	q_e
10	0.31	969	10	0.37	963
8	0.296	770.4	8	0.344	765.6
6	0.234	576.6	6	0.294	570.6
4	0.18	382	4	0.26	374
2	0.096	190.4	2	0.176	182.4

The Langmuir isotherm model can be expressed linearly in equation 4

$$\frac{1}{q_e} = \frac{1}{q_{max}} + \frac{1}{k_l q_{max}} \frac{1}{C_e} \qquad (4)$$

Where: C_e is the equilibrium concentration (mg/L), q_e is the amount adsorbed at equilibrium time mg/g. q_{max} and K_L are Langmuir constants which relate adsorption capacity and the energy of adsorption respectively. q_{max} and K_L can be obtained from the slope and intercept of the graph $\frac{1}{q_e}$ against $\frac{1}{C_e}$ ((Piccin, *et al.,* 2011)).

The plots of $1/q_e$ versus $1/C_e$ (Figure 4) for both H_2SO_4 and $ZnCl_2$ activated carbon adsorbents gave a straight line with $1/q_{max}$ as intercept and $1/K_L q_{max}$ as slope, and hence q_{max} and K_L were estimated (Table 3). For the Langmuir model, the constants K_L is the adsorption equilibrium constant (mg/L) and q_{max} is the monolayer adsorption capacity of the adsorbent (mg/g).
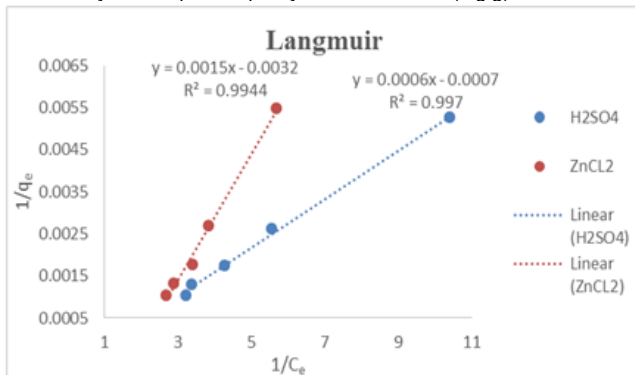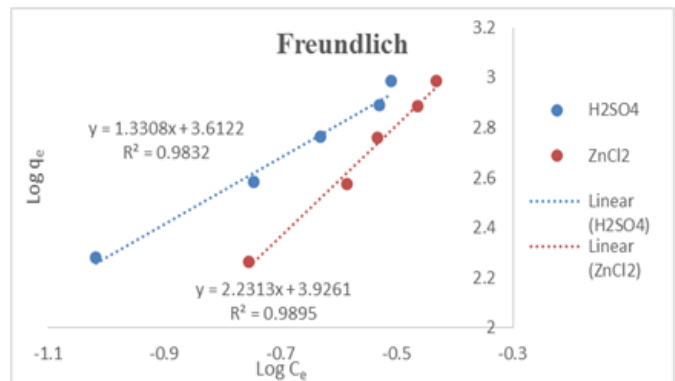

Figure 4: Langmuir adsorption isotherm linear plot of methylene blue adsorption by OP-AC activated with H_2SO_4 and $ZnCl_2$

The q_{max} value obtained from the linear Langmuir plot for Methylene blue adsorption with H_2SO_4 and $ZnCl_2$ activated orange peel activated carbons (Figure 4) was 1428.5714 and 312.5 mg/g respectively.

Furthermore, the essential characteristics of the Langmuir isotherms can be described by a separate dimensionless factor R_L. If R_L is greater than 1 then the adsorption is unfavourable, if R_L is less than 1 but greater than 0 then it is favourable, if R_L is equal to 1 then the adsorption is Linear and if it is equal to 0 the adsorption

is irreversible. According to Table 3, the R_L for adsorption of MB for both H_2SO_4 and $ZnCl_2$ activated carbons are greater than 0 but less than 1 indicating that the adsorption according to the Langmuir adsorption studies was favourable.

The Langmuir isotherm model appeared to be more applicable to the adsorption studies than Freundlich model as it was observed to have the highest R^2 value for both H_2SO_4 and $ZnCl_2$ activated carbons. Similar studies for the removal of methylene blue dye with activated carbon from waste tobacco stalks, common fig seeds, water melon rinds, and banana peels were also observed to obey the Langmuir model (Henry *et al.,* 2017; Pathania *et al.,* 2017; Ngoh *et al.,* 2018; Jawad *et al*., 2018) for the removal of methylene blue dye. It can be deducted from the fitness of the Langmuir model to the adsorption process that the adsorbate ion molecules from the bulk solution were adsorbed on a specific monolayer.

Figure 5: Freundlich adsorption isotherm linear plot of methylene blue adsorption by OP-AC activated with H_2SO_4 and $ZnCl_2$

3.4.2 Freundlich Isotherm
Freundlich isotherm can be expressed linearly as:

$$\log_{10} q_e = \log_{10} K_f + \frac{1}{n} \log_{10} C_e \qquad (5)$$

As shown in Figure 5, the plot of log q_e vs log C_e for H_2SO_4 and $ZnCl_2$ orange activated carbons gave a straight line. The numerical values of the constants n and K_f of the plots were also calculated from the slope and intercept of the plots and presented in Table 3. The K_f values also showed that MB had a good affinity for OP-AC (Garba *et al.*, 2018). The other Freundlich constant, n, is a measure of the deviation of the adsorption from linearity. If the value of n is equal to unity, the adsorption is linear. If the value of n is below unity, it implies that the adsorption process is unfavourable, and if the value of n is above unity, adsorption is favourable (Roulia & Vassiliadis, 2008). As shown is Table 3, the values of the constant 'n' for the both adsorption studies were higher than unity implying that the adsorption process was favourable and also a physical process. The Freundlich model was observed to have a significantly high R^2. Similar studies for the removal of methylene blue dye with activated carbon from black cumin seeds and coconut shells activated with sulphuric acid were observed to obey the Freundlich model (Thabede *et al.,* 2020; Jawad *et al*. 2020).

Table 3: Parameters obtained from Langmuir and Freundlich adsorption Isotherms

Isotherm	Parameters	H_2SO_4	$ZnCl_2$
Langmuir	q_{max} (mg/g)	1428.5714	312.5
	K_L (L/mg)	1.1666667	2.133333
	R_L	0.0789474	0.044776
	R^2	0.997	0.9944
Freundlich	K_f (L/mg)	4094.4917	8435.29
	n	0.7514277	0.448169
	R^2	0.9832	0.9895

3.4.3 Adsorption Kinetics

Adsorption kinetics is a curve (or line) that describes the rate of retention or release of a solute from an aqueous environment to solid-phase interface at a given adsorbents dose, temperature, flow rate and pH (Kajjumba *et al.,* 2018). Adsorption kinetics measures the adsorption uptake with respect to time at constant concentration. The mechanism of the adsorption process was determined using pseudo-first-order and pseudo-second-order models.

Table 4: Adsorption kinetic studies for the removal of methylene blue by OP-AC activated with H_2SO_4 and $ZnCl_2$ sample

|	H_2SO_4				$ZnCl_2$			
Time	C_o	C_t	q_t	q_e-q_t	C_o	C_t	q_t	q_e-q_t
0	10	4.04	596	373	10	5.44	456	507
30	10	0.57	943	26	10	0.91	909	54
45	10	0.5	950	19	10	0.69	931	32
60	10	0.44	956	13	10	0.58	942	21
75	10	0.38	962	7	10	0.39	961	2

3.4.4 Pseudo first-order

The Lagergren equation is used to express the pseudo-first-order model, which posits that the rate of adsorption site occupation is proportional to the number of unoccupied sites and it is given by:

$$\ln(q_e - q_t) = \ln q_e - K_1 t \qquad (6)$$

Where q_e and q_t are the amount of Methylene Blue adsorbed (mg/g) at equilibrium and at any time t, respectively, k_1 (min⁻¹) is the rate constant of pseudo-first-order model, and t is the time (min). A plot of $\ln(q_e - q_t)$ versus t is used to estimate the values of k_1 and q_e from the slope and the intercept, respectively.

The R^2 of the plots of the Pseudo First order of H_2SO_4 and $ZnCl_2$ activated carbons were determined to be 0.9108 and 0.9334 respectively as presented in Table 5. Also the calculated q_e values (233.52754 mg/g and 531.9237 mg/g) for MB adsorption onto H_2SO_4 and $ZnCl_2$ OP-AC activated carbons of the Pseudo first-order kinetics reactions were found to differ significantly from the experimental q_e values of 969 mg/g and 963 mg/g respectively. This proves the inapplicability of the pseudo first-order to the adsorption kinetics reaction.
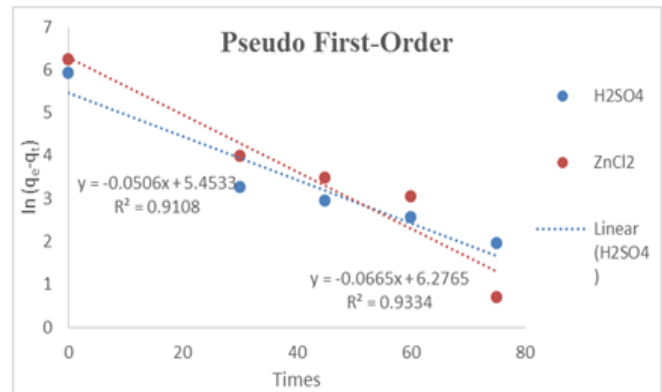
Figure 6: Pseudo first-order linear plot of methylene blue adsorption by OP-AC activated with H_2SO_4 and $ZnCl_2$
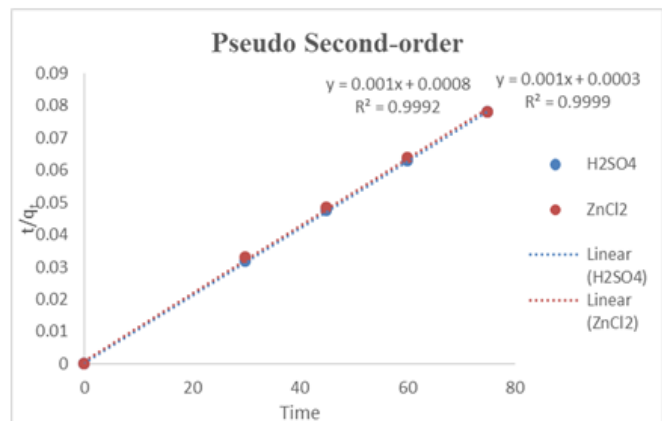
Figure 7: Pseudo second-order linear plot of methylene blue adsorption by OP-AC activated with H_2SO_4 and $ZnCl_2$

3.4.5 Pseudo Second-order

The pseudo-second-order kinetic model can be expressed in the linear form as follows:

$$t/q_t = \frac{1}{K_2} q_e^2 + \frac{1}{q_e} \qquad (7)$$

Where K_2 is the equilibrium rate constant of pseudo-second-order model (g/mg min⁻¹). The values of q_e and K_2 can be determined from the slope and intercept of the plot of (t/q_t) versus t respectively. The Pseudo Second-order was observed to have significantly higher R^2 values (0.9999) for both H_2SO_4 and $ZnCl_2$ activated carbons than the Pseudo First-order. Also the calculated q_e OP-AC adsorbent (1000 mg/g) for both adsorbents was observed to be closer in value to the experimental q_e values of 969 mg/g and 963 mg/g respectively, further confirming the fitness of Pseudo Second-order for the adsorption of MB ions onto H_2SO_4 and $ZnCl_2$ activated OP-AC.

Table 5: Adsorption kinetics parameters from the Pseudo first and second-order plots

	Parameters	H_2SO_4	$ZnCl_2$
Pseudo-first-order	qe cal. (mg/g)	233.52754	531.9237
	qe exp. (mg/g)	969	963
	K_1	0.000675	0.000887
	R^2	0.9108	0.9334
Pseudo-second-order			
	qe cal. (mg/g)	1000	1000
	qe exp. (mg/g)	969	963
	K_2	3.3333333	1.25
	R^2	0.9999	0.9992

Conclusion

Activated carbon was prepared from waste Orange peel using H_2SO_4 and $ZnCl_2$ activating agents. Activated carbon with $ZnCl_2$ activating agent produced better yield when compared to activated carbon with H_2SO_4 activating agents. SEM and FTIR showed that activated carbon with micropores were successfully synthesized. Adsorption studies revealed the adsorption of methylene blue dye onto the adsorbents with H_2SO_4 activated carbon performing slightly better than $ZnCl_2$ activated carbon. Both H_2SO_4 and $ZnCL_2$ OP-AC samples showed favourable adsorption with better fit of R^2 = 0.997, 0.994 (H_2SO_4, $ZnCL_2$) and 0.9832, 0.9895 (H_2SO_4, $ZnCL_2$) for Langmuir and Freundlich respectively. The adsorption process was determined to be a physical and favorable adsorption. The rate of adsorption for both adsorbents was determined to be pseudo-second order. Activated carbon prepared from orange peels can be utilized in the removal of methylene blue dye from solution and waste water.

REFERENCES

Egbosiuba, T. A., Kovo, A., Afolabi, E., Tijani, J., Auta, M., & Roos, W. (2020). Ultrasonic enhanced adsorption of methylene blue onto the optimized surface area of activated carbon: Adsorption isotherm, kinetics and thermodynamics. *Chemical engineering research and design, 153*, 315-336.

Evwierhoma, E., Madubiko, O., & Jaiyeola, A. (2018). Preparation and characterization of activated carbon from bean husk. *Nigerian Journal of Technology, 37*(3), 674-678.

Garba, Z. N., Okibe, F. G., & Alimi, J. M. (2018). Optimization of the conditions for adsorption of fluoride in aqueous solution by carrot residue using central composite design of experiment. *Bayero Journal of Pure and Applied Sciences, 11*(1), 230 - 237.

Gavahian, M., Chu, Y., & Khaneghah, A. M. (2019). Recent advances in orange oil extraction: An opportunity for the valorisation of orange peel waste a review. *International Journal of Food Science & Technology, 54*(4), 925-932.

Henry, M., Lilian, T., david, M., & M, B. (2017). Methylene blue removal using a low cost activated carbon adsorbent from tobacco stems: kinetic and equilibrium studies. *Water Science and Technology, 75*, 2390-2402.

Islam, M., Sabar, S., Benhouria, A., Khanday, W., Asif, M., & Hameed, B. (2017). Nanoporous activated carbon prepared from karanj (Pongamia pinnata) fruit hulls for methylene blue adsorption. *Journal of the Taiwan Institute of Chemical Engineers, 74*, 96-104.

Jawad, A., Ramlah, A., Mohd, A., & Ismail, K. (2018). Adsorptive removal of methylene blue by chemically treated cellulosic waste banana (Musa sapientum) peels. *Journal of Taibah University for Science, 12*.

Jawad, A., Rashid, R., Ishak, M., & Wilson, L. (2016). Adsorption of methylene blue onto activated carbon developed from biomass waste by H2SO4 activation: kinetic, equilibrium and thermodynamic studies. *Desalination and Water Treatment, 57*(52), 25194-25206.

Jawad, H., Saud, A., & Mohd, M. (2020). Acid factionalized biomass material for methylene blue dye removal: a comprehensive adsorption and mechanism study. *Journal of Taibah University for Science, 14*, https://doi.org/10.1080/16583655.2020.1736767.

Kajjumba, G. W., Emik, S., Öngen, A., Kurtulus, H. Ö., & Serdar, A. (2018). Modelling of Adsorption Kinetic Processes - Errors, Theory and Application. In *Advanced Sorption Process Applications* (p. DOI: http://dx.doi.org/10.5772/intechopen.80495).

Martín, M., Siles, J., Chica, A., & Martín, A. (2010). Biomethanization of orange peel waste. *Bioresource technology, 101*(23), 8993-8999.

Ngoh, Y., Ali, H., & Radzun, A. (2018). Utilization of watermelon (Citrullus lanatus) rinds as a natural low cost biosorbent for adsorption of methylene blue: kinetic, equilibrium and thermodynamic studies. *10*, https://doi.org/10.1080/16583655.2018.1476206.

Özsin, G., Kılıç, M., Apaydın-Varol, E., & Pütün, A. (2019). Chemically activated carbon production from agricultural waste of chickpea and its application for heavy metal adsorption: equilibrium, kinetic, and thermodynamic studies. *Applied water science, 9*, 1-14.

Pallarés, J., González-Cencerrado, A., & Arauzo, I. (2018). Production and characterization of activated carbon from barley straw by physical activation with carbon dioxide and steam. *Biomass and bioenergy, 115*, 64-73.

Pathania, D., Sharma, S., & Singh, P. (2017). Removal of methylene blue by adsorption onto activated carbon developed from Ficus carica bast. *Arabian Journal of Chemistry, 10*, 1445-1451.

Piccin, J. S., Dotto, G. L., & Pinto, L. A. (2011). Adsorption isotherms and thermochemical data of fd&c red n° 40 binding by chitosan. *Brazilian Journal of Chemical Engineering, 28*(2), 295 - 304.

Roulia, M., & Vassiliadis, A. A. (2008). Sorption, characterzation of catiomic dye retained by clays and perlite. *Microporous and Mesoporous Materials, 116*, 732-740.

Santos, C., Dweck, J., Viotto, R., Rosa, A., & de Morais, L. (2015). Application of orange peel waste in the production of solid biofuels and biosorbents. *Bioresource Technology, 196*, 469-479.

Sugumaran, P., Susan, V., Ravichandran, P., & Seshadri, S. (2012). Production and characterization of activated carbon from banana empty fruit bunch and Delonix regia fruit pod. *Journal of Sustainable Energy & Environment, 3*(3), 125-132.

Thabede, M., Ntaote, D., & Eliazer, N. (2020). Removal of methylene blue and lead ions from aqueous solution using activated carbon from black cumin seeds. *South African Journal of Chemical Engineering, 33*, 39-50.

Ünal, G., Gülce, Ö., & Gizem, Ç. G. (2013). Removal of methylene blue from aqueous solution by activated carbon prepared from pea shells (pisum sativum). *Journal of Chemistry*,

https://dx.doi.org/10.4314/swj.v18i3.25

http://dx.doi.org/10.1155/2013/614083.

Wibawa, Pratama, J., Muhammad, N., Mukhamad, A., & Hadi, N. (2020). SEM, XRD and FTIR analyses of both ultrasonic and heat generated activated carbon black microstructures. *Heliyon , 6*(3).

Wyasu, G. (2020). Batch adsorption of Hg2+ and As3+ ions in Hospital wastewater using activated carbon from Balanites aegyptiaca and Detarium microcarpum. *Communication in Physical Sciences, 5*(4).

Xue, H., Wang, X., Xu, Q., Dhaouadi, F., Sellaoui, L., Seliem, M., . . . Li, Z. (2022). Adsorption of methylene blue from aqueous solution on activated carbons and composite prepared from an agricultural waste biomass: A comparative study by experimental and advanced modeling analysis. *Chemical engineering journal, 430*, 132801.

Yusufu, M., Ariahu, C., & Igbabul, B. (2012). Production and characterization of activated carbon from selected local raw materials. *African journal of pure and applied chemistry, 6*(9), 123-131